1988

Secondary Current Distributions Using TOPAZ2D and Linear Kinetics

E. C. Dimpault-Darcy
Texas A & M University - College Station

Ralph E. White
University of South Carolina - Columbia, white@cec.sc.edu

Publication Info

Journal of the Electrochemical Society, 1988, pages 656-658.

http://www.electrochem.org
DOI: 10.1149/1.2095692
http://dx.doi.org/10.1149/1.2095692

and necessarily has a "noisy" current signal), (*ii*) all of the limiting current density experiments were performed using baths whose density and kinematic viscosity had been measured, or (*iii*) the limiting current density "plateau" for the EDTA baths was more extensive (adsorption of Quadrol (4) apparently decreases the potential region for the mass transport-controlled reaction).

Acknowledgments

This material is based upon work supported by the National Science Foundation under Grants no. ENG7511869 and no. ENG7909745. One of the authors (R.Y.Y.) received a Hooker Chemicals and Plastics Corporation Summer Research Fellowship during part of this work. Quadrol samples were donated by BASF Wyandotte Corporation.

Manuscript submitted May 28, 1985; revised manuscript received Feb. 28, 1986. This was Paper 665RNP presented at the Denver, CO, Meeting of the Society, Oct. 11-16, 1981, and Paper 135 presented at the Detroit, MI, Meeting of the Society, Oct. 17-21, 1982.

The University of Michigan assisted in meeting the publication costs of this article.

REFERENCES

1. J. Dumesic, J. A. Koutsky, and T. W. Chapman, *This Journal*, **121**, 1405 (1974).
2. F. M. Donahue, *ibid.*, **127**, 51 (1980).
3. F. M. Donahue, K. L. M. Wong, and R. V. Bhalla, *ibid.*, **127**, 2340 (1980).
4. F. M. Donahue, D. J. Sajkowski, A. C. Bosio, and L. L. Schafer, *ibid.*, **129**, 717 (1982).
5. F. L. Shippey and F. M. Donahue, *Plating*, **60**, 43 (1973).

Secondary Current Distributions Using TOPAZ2D and Linear Kinetics

E. C. Dimpault-Darcy* and R. E. White**

Department of Chemical Engineering, Texas A&M University, College Station, Texas 77843-3122

Secondary current density distributions are of interest to cell designers. The purpose of this note is to illustrate how to use an existing numerical method to determine these distributions for cells that contain conducting and nonconducting bodies between the main anode and cathode.

The method is based on a public domain heat transfer code called TOPAZ2D (1). The finite element based method allows for jump changes in the potential from one region to another within the field of interest. This feature is unique and is important for modeling stacks of bipolar plate cells, cathodic protection systems, electrodeposition, and other systems where the designer does not have control of the potential (or current) in regions inside the cell.

The method is used here to show how to extend the model of a stack of bipolar plate cells that was presented earlier by Holmes and White (2). In their work, they neglected surface overpotentials which are defined here as the difference between the potentials at an interface between two regions (A and B) at which an electrochemical reaction occurs

$$\eta = \phi_A - \phi_B \qquad [1]$$

This expression requires special mathematical treatment because the two potentials coincide spatially, as discussed briefly below.

Others (3, 4) have presented methods for including surface overpotentials with the boundary element method and the finite element method. Deconinck *et al.* (3) included surface overpotentials at the electrode surfaces in their two-electrode cell model using a boundary element technique, and Tokuda *et al.* (4) included surface overpotential in their finite element method. Unfortunately, both methods require that the electrode surfaces lie on the boundaries of the cell, where one of the potentials in Eq. [1] can be set. This restriction makes their methods inappropriate for modeling stacks of bipolar plate electrochemical cells.

Model and Solution Method

A stack of bipolar plate cells is shown in Fig. 1. Assuming uniform concentration, the two-dimensional Laplace equation

$$\frac{\partial}{\partial x}\left(K_x \frac{\partial \phi}{\partial x}\right) + \frac{\partial}{\partial y}\left(K_y \frac{\partial \phi}{\partial y}\right) = 0 \qquad [2]$$

governs the potential in the conducting regions in the cells (electrolyte and bipolar plates). In this work, the electrical conductivity is assumed to be isotropic ($K_x = K_y$), and the symbols, κ and σ, are used to denote the conductivity of the electrolyte and the bipolar plates, respectively. In the previous model (2), the potentials at the terminal anode and cathode are set. This condition is used for predicting primary current distributions in which the surface overpotential concept is neglected. That is, the potential of the electrolytic solution adjacent to the electrodes is assumed to be equal to the electrode potential and is thus an equipotential surface. This assumption is reasonable only if the electrode kinetics are very fast, or if the current density is very low.

At an interface between a solid electrode and an electrolyte, the surface overpotential can be defined as

$$\eta(x,y) = \phi_{solid}(x,y) - \phi_{solution}(x,y) \qquad [3]$$

where ϕ_{solid} is the potential on an electrode surface and $\phi_{solution}$ is the potential of the electrolytic solution adjacent to the surface of the solid electrode. For small surface overpotentials, Newman (5) gives a simplified linear relationship between the overpotential and the normal derivative of the potential

$$i_n = (\alpha_a + \alpha_c)\frac{i_o \mathbf{F}}{RT}\eta = -\kappa \frac{\partial \phi}{\partial n} \qquad [4]$$

Using TOPAZ2D to solve this electrochemical problem requires a transformation to dimensionless variables. Consequently, let

$$\Phi = \frac{\mathbf{F}}{RT}\phi, \qquad X = \frac{x}{l}, \qquad \text{and} \qquad Y = \frac{y}{t} \qquad [5]$$

where l is the half-length of the cells and t is the height of the stack. Using Eq. [3], [4], and [5], Eq. [2] becomes dimensionless, and for Fig. 1, the resulting external boundary conditions are

$$\frac{\partial \Phi}{\partial Y} = (\alpha_a + \alpha_c)\frac{i_o t \mathbf{F}}{\kappa RT}[\Phi_{anode} - \Phi(X,1)] \qquad [6]$$

at the top anodic plate and

$$\frac{\partial \Phi}{\partial Y} = -(\alpha_a + \alpha_c)\frac{i_o t \mathbf{F}}{\kappa RT}[\Phi_{cathode} - \Phi(X,0)] \qquad [7]$$

*Electrochemical Society Student Member.
**Electrochemical Society Active Member.

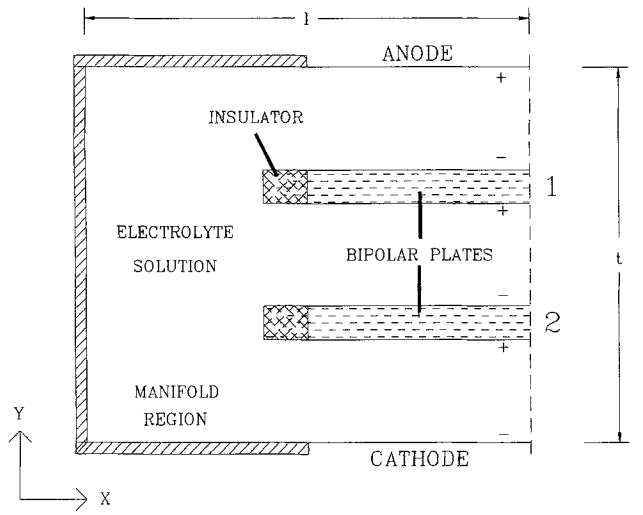

Fig. 1. Bipolar plate cell model

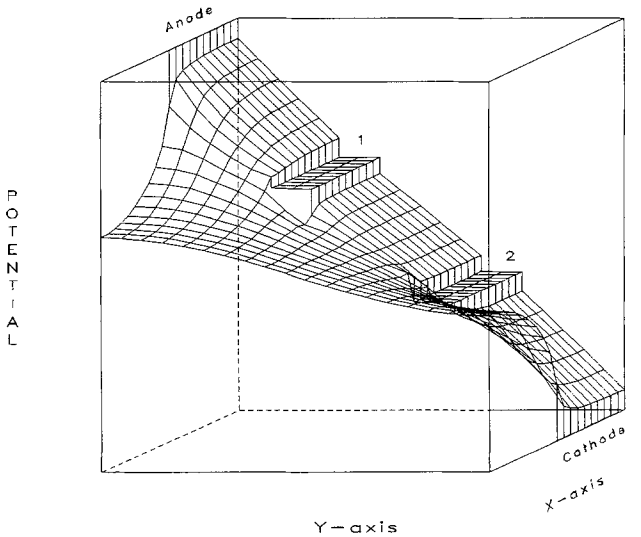

Fig. 3. Potential distribution plot for the model shown in Fig. 1 subject to the parameters given in Table I.

at the bottom cathodic plate. The dimensionless potential at the anode, Φ_{anode}, and at the cathode, $\Phi_{cathode}$, are specified constants. Equations [6] and [7] have simple heat transfer analogs since they resemble convection-type boundary conditions

$$\frac{\partial T}{\partial y} = h(T - T_\infty) \qquad [8]$$

In a similar fashion to Eq. [6] and [7], the cathode sides of the bipolar plates are governed by

$$\frac{\partial \Phi_{solution}}{\partial Y} = -(\alpha_a + \alpha_c)\frac{i_o t \mathbf{F}}{\kappa RT}[\Phi_{solid}(X,Y) - \Phi_{solution}(X,Y)] \qquad [9]$$

and the anode sides of the bipolar plates are governed by Eq. [9] with a sign change. Such expressions are difficult to model since they contain two unknowns which, by neglecting the double layer, conceptually coincide spatially. A novel feature of TOPAZ2D enables it to handle Eq. [9] through its heat transfer analog equation

$$\frac{\partial T}{\partial y} = h_c(T_A - T_B) \qquad [10]$$

for a thermal contact resistance across an interface between mediums A and B. TOPAZ2D uses internal boundary elements to allow thermal coupling between two surfaces as indicated in Fig. 2. While four nodes (N_{A_1}, N_{A_2}, N_{B_1}, and N_{B_2}) are required to define this element, opposed nodal coordinates (*i.e.*, N_{A_1} and N_{B_1}) may coincide, reducing the gap to zero. In the electrochemical problem, A corresponds to the electrolyte, and B represents the adjacent electrode surface. Comparison of Eq. [9] and [10] shows that the heat transfer analog can be completed by defining a dimensionless surface overpotential coefficient

$$\beta = (\alpha_a + \alpha_c)\frac{i_o t \mathbf{F}}{\kappa RT} \qquad [11]$$

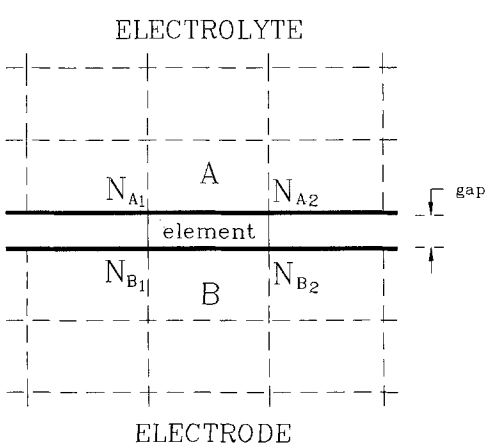

Fig. 2. Schematic of an internal boundary element

Results and Discussion

Figure 3 presents the potential distribution for the stack of bipolar plate cells of Fig. 1 with the set of parameters in Table I. The profile was obtained by using TOPAZ2D to solve Laplace's equation (Eq. [2]) in both the electrolyte and bipolar plates of Fig. 1. The profile between the bipolar plates follows the expection of Pletcher (6). Current flows from the anode through the electrolyte and the bipolar plates to the cathode. Most of the potential drop occurs in the electrolyte due to the relatively low conductivity of the electrolytic solution. Unlike the previous model (2), the insulators at the end of the plates do not lie in the model domain and are represented by internal blank regions in the surface plot. This method treats the internal insulators like boundary insulators that have an infinite resistance to current flow. Some current bypasses the bipolar plate region and flows around the insulators through the electrolyte in the manifold region. The sharp and abrupt potential jump at the surfaces of the electrodes represents the surface overpotential. Note also that the solution adjacent to the electrode surface is clearly not an equipotential surface, as assumed before (2). It should be noted that the geometry shown in Fig. 1 was chosen for demonstration purposes. A more realistic design would have included larger insulators at the ends of the bipolar plates. The selected geometry produces a more prominent bypass current which results in a more apparent variance in the overpotential along the electrode surface. Accounting for variances in overpotential is important because it allows designers to better predict the level of nonuniformities in potential distribution in their designs.

In closing, this electrochemical problem could possibly be handled by other finite element heat transfer codes (7). However, TOPAZ2D's internal boundary element feature

Table I. Parameters values

Φ_{anode}	1.0
$\Phi_{cathode}$	0.0
κ (Ω^{-1} cm^{-1})	0.0001
σ (Ω^{-1} cm^{-1})	0.01
β	0.001

is simple and direct. It should be possible to incorporate Butler-Volmer kinetics, or any similar relation, into TOPAZ2D by altering the portion of the code dealing with convection-type boundary conditions and with the internal boundary element conditions for coupling interfacial surfaces. Also, TOPAZ2D can be used to calculate fluxes at each nodal point to give the current density distribution. In addition, a three-dimensional version of the code, TOPAZ3D, has been developed (8).

Manuscript submitted Dec. 29, 1986; revised manuscript received July 22, 1987.

Texas A&M University assisted in meeting the publication costs of this article.

LIST OF SYMBOLS

$\mathbf{F}$	Faraday's constant, 96,487 C/mol of electrons
h	convection heat transfer coefficient, W/m^2 K
h_c	contact resistance heat transfer coefficient, W/m^2 K
i_n	normal component of the current density vector, A/cm^2
i_o	exchange current density at equilibrium, A/cm^2
K_x	electrical conductivity in the x-direction, Ω^{-1} cm^{-1}
K_y	electrical conductivity in the y-direction, Ω^{-1} cm^{-1}
l	horizontal half-length of bipolar plate cells, cm
n	unit normal vector, cm
N	element node number
R	universal gas constant, 8.3143 J/mol K
T	absolute temperature, K
T_A	temperature in region A, K
T_B	temperature in region B, K
t	vertical height of the stack of bipolar plate cells, cm
x	horizontal spatial coordinate, cm
y	vertical spatial coordinate, cm
X	dimensionless horizontal spatial coordinate
Y	dimensionless vertical spatial coordinate

Greek symbols

α_a	transfer coefficient in the anodic direction
α_c	transfer coefficient in the cathodic direction
β	dimensionless surface overpotential coefficient
κ	electrical conductivity of electrolytic solution, Ω^{-1} cm^{-1}
η	overpotential at electrode surface, V
ϕ	potential, V
ϕ_A	potential in region A, V
ϕ_B	potential in region B, V
Φ	dimensionless potential
Φ_{anode}	dimensionless potential at the anodic surface of electrode
$\Phi_{cathode}$	dimensionless potential at the cathodic surface of electrode
Φ_{solid}	dimensionless potential of solid electrode surface
$\Phi_{solution}$	dimensionless potential of electrolyte
σ	electrical conductivity of solid electrode, Ω^{-1} cm^{-1}

REFERENCES

1. A. B. Shapiro, "TOPAZ2D; A Two-Dimensional Finite Element Code Heat Transfer Analysis, Electrostatic and Magnetostatic Problems," UCID-20824, Mechanical Engineering Department, Lawrence Livermore National Laboratory, July 1986.
2. J. W. Holmes and R. E. White, in "Electrochemical Cell Design," R. E. White, Editor, p. 311, Plenum Press, New York (1984).
3. J. Deconinck, G. Maggetto, and J. Vereecken, *This Journal*, **132,** 2960 (1985).
4. K. Tokuda, T. Gueshi, K. Oaki, and H. Matsuda, *ibid.*, **132,** 2390 (1985).
5. J. S. Newman, "Electrochemical Systems," p. 346, Prentice-Hall, Inc., Englewood Cliffs, NJ (1973).
6. D. Pletcher, "Industrial Electrochemistry," p. 77, Chapman and Hall, London (1982).
7. A. D. Noor, *Finite Elements in Analysis and Design,* **2,** 259 (1986).
8. A. B. Shapiro, "TOPAZ3D; A Three-Dimensional Finite Element Heat Transfer Code," UCID-20484, Mechanical Engineering Department, Lawrence Livermore National Laboratory, August 1985.

The Current Distribution on a Rotating Disk Electrode in Potentiostatic Pulsed Electrolysis

Haewei H. Wan* and Huk Y. Cheh**

Department of Chemical Engineering and Applied Chemistry, Columbia University, New York, New York 10027

A number of recent articles deal with pulsed potential electrolysis. For instance, Despic and Popov (1) studied mass transfer under pulsed potential conditions in the absence of convection. Viswanathan and Cheh (2) presented a mathematical model for mass transfer to a rotating disk electrode (RDE) by applying potentiostatic pulses. Gelchinski *et al.* (3) electroplated chromium-cobalt alloys by using a pulsed potential source. However, all these treatments were based on the assumption that the electrode surface received a uniform current. In a recent paper (4), we demonstrated the nonuniformity of current distribution under various pulsed current conditions. In this investigation, we show how the mathematical model developed by pulsed current technique can be extended to pulsed potential electrolysis. The differences between these two methods are also discussed.

By making the same model assumptions and nomenclature as in our previous paper (4), the concentration of the reacting species is governed by the following transient convective diffusion equation

$$\frac{\partial C}{\partial t} + v_r \frac{\partial C}{\partial r} + v_z \frac{\partial C}{\partial z} = D \frac{\partial^2 C}{\partial z^2} \qquad [1]$$

with the boundary conditions

$$C = C_\infty, \text{ at } t = 0 \text{ and for all } r \text{ and } z \qquad [2]$$

$$C = C_\infty, \text{ at } t > 0 \text{ and for } r^2 + z^2 \to \infty \qquad [3]$$

$$-D \frac{\partial C}{\partial z} = \frac{i}{n\mathbf{F}}, \text{ at } t > 0,\ z = 0, \text{ and for all } r \qquad [4]$$

$$\frac{\partial C}{\partial r} = 0, \text{ at } t > 0,\ r = 0, \text{ and for all } z \qquad [5]$$

During the on-period of the cycle, the applied potential on the disk V_t with a large copper counterelectrode is a constant, the sum of the ohmic potential drop Φ_0, the concentration overpotential η_c, and the surface overpotential η_s

$$V_t = \Phi_0 + \eta_c + \eta_s \qquad [6]$$

During the off-period of the pulse

$$V_t = 0 \qquad [7]$$

Similar treatments and solution procedures to those in Ref. (4) are applied to obtain the concentration profile and current distribution. The only difference in computation

*Electrochemical Society Student Member.
**Electrochemical Society Active Member.